PREDICTION OF AERODYNAMICS LIFT REDISTRIBUTION ON FLEXIBLE WING STRUCTURE USING TRANSONIC UNSTEADY AERODYNAMIC CODE - NTRANS

I Wayan Tjatra[1] , M. Kadar[2] , Dwi Rahmawati[3]
Computational Aeroelastic Group , Aerospace Engineering Department
Institute of Technology Bandung , Jl. Ganesha 10 , Bandung 40132 , Indonesia
e-mail : tjatra@aeronautics.pn.itb.ac.id

ABSTRACT

Aeroelastic analysis of lifting surface involves solving fluid and structural equations together. Such coupling procedure need an advanced computational structure mechanics for the development of structural model and advanced computational fluid dynamics for the solution of aerodynamics flow model. NASTRAN, a well known computer code for structural analysis, has an advanced structural modeling, but does not has the capability for solving aerodynamically nonlinear problems, such as aeroelasticity in transonic flow regimes.

A computationally efficient technique for the prediction of aerodynamic lift redistribution on flexible wing structure in transonic flow field is presented in this paper. The advance capability in structural modelling of finite element based software module is integrated with a newly developed NTRANS, unsteady transonic aerodynamic software module. This integration is carried out through a quasi - steady coupling of the aerodynamic generalized forces with the elastic structural deformation. This integration technique has been validated for clean wing configuration. Comparison of numerical results with results obtained using other numerical technique proves that this technique is accurate and efficient for routine application.

INTRODUCTION

Aerodynamics and structures interaction plays a critical rule in airframe design. It becomes even more significant when viewed in the context of emerging multidisciplinary design concept, because the accuracy of both the aerodynamic and structural models improves the reliability of the optimal solutions. This static and dynamic aeroelastic problem is govern by the mutual interaction of elastic and inertial forces of the structure with the steady and unsteady aerodynamic loading induced by the deformation or oscillation of part of the aircraft structure itself[1]. Aerodynamic lift – redistribution is one of the static aeroelastic phenomena in which the elastic deformation of a flexible structure cause a change in pressure distribution and, also , lift distribution on the surface of the structure. At the same time, a change in surface pressure distribution bring a change in structure deformation. Interaction between these two forces, the aerodynamic and elastic forces , has to be taken into account during the design process of a lifting surfaces structure. The significant of the aerodynamic pressure or lift redistribution increases with the increase of aerodynamic load and flow velocity. Special consideration has to be given for flow in transonic regime due to the presents of shock waves. In this regime, characteristics of the aerodynamic load is strongly nonlinear with large phase lag between structure deformation and the aerodynamic response. The interaction behavior in this aerodynamically nonlinear system will also be nonlinear.

At present time, there is a continuous effort to improve the performance of subsonic transport

[1] Assistant Professor , Aerospace Engineering Department , Member AIAA
[2] Engineer , Nusantara Aircraft Industry Ltd. , Indonesia
[3] Engineer , Nusantara Aircraft Industry Ltd. , Indonesia

aircraft. One attempt is to improve the fuel efficiency by extending the flight regime to high sub-transonic Mach numbers to increase lift-to-drag ratios and flight speed. But, an increase in Mach number into transonic regime will bring other important problems of high induced drag and nonlinear aeroelastic response phenomenon, which include nonlinear aerodynamic lift redistribution.

To accurately predict the nonlinear characteristic of this aerodynamic lift redistribution at transonic speed, it is necessary to model the flows with an appropriate flow equation or system of equations. Navier - Stokes equations are capable of presenting mathematically the physical phenomena encountered in most of fluid dynamic problems such as transonic flows, including shock waves , boundary layers and the shock waves – boundary layer interaction . This flow equations consists of system of nonlinear, second order partial differential equation in space and time. Its numerical solution requires the implementation of the tangency boundary condition on the body surface, for which a time dependent, body conforming grid system have to be used. This requirement adds the overall complexity and computational effort and resources of the problem. Consequently a simpler form of equation, but still can describe a typical transonic flow structure, is often utilized. At present time, transonic small disturbance (TSD) equation is widely used in the prediction of unsteady aerodynamic loads for aeroelastic analysis, besides several older linearized aerodynamic theory that had been developed 30 years ago, such as: Doublet - Lattice and Vortex - Lattice theory, quasi steady Mach Box theory and unsteady Piston theory. Most of these linearized aerodynamic theory, however, can not directly taking into account several important parameters such as: lifting surface thickness and camber, angle of incidence and oscillation amplitude and frequency[2] Some empirical corrections procedure to these theory have been developed and used for routine aircraft design purposes.

NASTRAN, a well known and widely use computer code today for aeroelastic design and analysis, was developed based upon uncoupled aeroelastic solution procedure. Structural equation of motions is solved using the finite element discretization method. Meanwhile, the aerodynamic loads working on the structure are calculated using a linearized aerodynamic theory such as Doublet - Lattice method and Mach Box theory. The linearized aerodynamic theories being used could accurately predict the aerodynamic load only for flow in low subsonic or high supersonic regimes. Outside these flow regimes, where the flow nonlinearities increases, significant error in the prediction of the aerodynamic load may occurs

The most advanced procedure for nonlinear transonic aeroelastic analysis commonly used at present time are based on the TSD theory, such as ATRAN3S and CAP-TSD (both developed at NASA Langley and is limited for US company use only). ATRAN3S code, NASA Ames version of XTRAN3S, is a three-dimensional code based upon a time-accurate, finite difference methods using alternating direction implicit (ADI) algorithm. Several terms of the ADI algorithm used in this code treated explicitly, which leads to time steps restriction based upon numerical stability consideration. Therefore, it is becomes very expensive for three-dimensional applications not just because of the small time-step needed to obtain convergence results, but also because not all sweep in the algorithm can be written in vectorized form [5]. Meanwhile, an approximate factorization (AF) algorithm [6] that is applied in CAP-TSD was proven to be more efficient for three-dimensional calculations. This AF algorithm consists of a time-linearization procedure coupled with a Newton iteration technique. In this algorithm, the Newton iteration process occupied most of the computing time needed. Even though both ATRAN3S and CAP-TSD computer code are much faster compared to Navier-Stokes or Euler based code , their use for design and analysis is still considered to be expensive and is limited only for analysis during the final design stage of an aircraft.

The main objective of this work is to developed an integration procedure between transonic aerodynamic load prediction module called NTRANS (Nusantara TRANSonic) and a linear finite element module for prediction of structure deformation called NFLEX. The NTRANS code was developed based upon the solution of TSD flow equations using modified AF algorithm which has higher efficiency and accuracy compared to the original scheme[3]. From previous study, it was found that Newton iteration step employed in the original AF algorithm is the major source of the slow convergence. Features that distinguished this new solution procedure from the other solution techniques are the implementation of a cyclic acceleration technique[5] for improvement in convergence rate. In this technique an acceleration coefficient, α, with cyclic values is added during the sweeping process in the chordwise direction. The addition of this coefficient will gives stable and accurate results with less iteration number per time step.

Integration of NTRANS and NFLEX are carried out in a quasi – steady fashion in which the time history of the structure's aerodynamic response are neglected. Numerical results for a clean wing configuration at subsonic and transonic speed regimes shows that this algorithm is accurate and efficient for routine design use.

AERODYNAMIC MODEL

NTRANS computer code is developed based upon the linearized parabolic transonic flow equations, which is the modified transonic small disturbance equation. The transonic small disturbance equation is obtained by combining the continuity and Bernoulli equation for a perfect gas with the isentropic flow relation and written in conservation form as

$$\frac{\partial f_o}{\partial t}+\frac{\partial f_1}{\partial x}+\frac{\partial f_2}{\partial y}+\frac{\partial f_3}{\partial z}=0 \qquad [\,1\,]$$

where t is the nondimensional time $= k\,\bar{t}$ with k represent the oscillation reduced frequency. The f_o, f_1, f_2 and f_3 coefficients are defined, in term of the disturbance velocity potential , as follows :

$$f_o = -B\phi_x + A\phi_t \;,\; f_1 = E\phi_x + F\phi_x^2 + G\phi_y^2$$

$$f_2 = \phi_y + H\phi_x\phi_y \;,\; f_3 = \phi_x$$

where A , B , F , G and H coefficients are function of free stream Mach number, motion reduced frequency and specific heat coefficients. Complete definition can be found in reference 3. The pressure coefficient on the lifting surface, expressed in terms of the perturbation potential velocity, are calculated from the relation

$$C_p = -2\phi_x - 2\phi_t - (1-M^2)\,\phi_x^2 - \phi_y^2 \qquad [\,2\,]$$

The cubical and higher powers of the perturbation velocity in the above relation are neglected.

Numerical computations are carried out in computational domain, within a rectangular region conform to the body, which is obtained by a coordinate transformation of the physical domain. The physical grid system in the (x, y, z) - plane is transformed into some (ξ,η,ζ) - plane, so that the mesh spacing in all directions can be kept uniform in the computational domain, using trigonometric and / or exponential transformation function. The flow boundary conditions that are imposed on the far-field (outer) boundary are similar to the nonreflecting boundary conditions introduced by Kwak[7] and the flow tangency conditions on the surface are applied on the mean plane of the oscillating surface, which is located along the axis parallel to the streamwise direction, z = 0, equidistantly between two horizontal gridlines. For unsteady flow calculations based upon the TSD equation, the surface tangency boundary conditions need not to be applied on the actual surface. Instead, it is applied on the mean plane of the body. Therefore, a body-fitted grid system is not required.

APPROXIMATE FACTORIZATION ALGORITHM

A modified Approximate Factorization (AF) algorithm is used for the solution of the flow equation, Eq. [1] . This scheme consists of a time linearization, to determine an estimate value of the perturbation potential, coupled with a Newton iteration technique to provide time accuracy in the solution. In this algorithm, flow equation is represented as triple product of differential operator, which is

$$L_\xi \, L_\eta \, L_\zeta \left(\Delta\phi \right) = R\left(\phi^*, \phi^n, \phi^{n-1}, \phi^{n-2} \right) \qquad [3]$$

where L_ξ, L_η, L_ζ represent differential operators in the ξ, η, ζ direction , respectively , $\Delta\phi$ is the error in the perturbation potential velocity , R represent residual of the equation , ϕ^* is the estimate value of the perturbation potential velocity , and $\phi^n, \phi^{n-1}, \phi^{n-2}$ is the perturbation velocity potential at time level n , (n-1) and (n-2) , respectively. The definition of L_ξ, L_η, L_ζ operators and R can be found in reference 3.

Equation [3] is solved through three - sweeps in the computational domain by sequentially applying the differential operators L_ξ, L_η, L_ζ as follows

$$\begin{aligned} \xi - \text{sweep} &: \quad L_\xi \, (\Delta\tilde{\phi}) = -R \\ \eta - \text{sweep} &: \quad L_\eta \, (\Delta\bar{\phi}) = \Delta\tilde{\phi} \qquad [4] \\ \zeta - \text{sweep} &: \quad L_\zeta \, (\Delta\phi) = \Delta\bar{\phi} \end{aligned}$$

Once these entire three sweeps completed, the updated values of ϕ at each grid points are computed by applying the last values of $\Delta\phi$ into the previous perturbation potential velocity:

$$\phi^{n+1} = \phi^* + \Delta\phi \equiv \phi^*_{new} \qquad [5]$$

The computation is started with an estimate value of ϕ^* and is carried out until a convergence solution of ϕ^{n+1} is obtained (until the perturbation error $\Delta\phi$ reaches the values of 10^{-6}). In most of the computation that had been performed [10], a maximum of 3 Newton iteration is needed for convergence solution at each time step.

Using the new ϕ^{n+1} values, the time linearization step is carried through to obtained the new estimate values of ϕ^* for the iteration of the next time step. In this step, the body surfaces are put at their new position and updated surface boundary conditions are applied. The unsteady solution are initiated using the steady solution as the first estimate values. Since the solution at each sweep depends entirely on the values that have been computed at the previous sweep, all sweeps can be coded in vectorized form.

CYCLIC ACCELERATION TECHNIQUE

Since all terms in this scheme are treated implicitly, this scheme does not have a time step restriction. In steady flow calculation and during the Newton iteration step in unsteady flow calculation, however, it is possible to accelerate the convergence rate of the procedure. This can be achieved by adding an a cyclic acceleration coefficient, α, into the right hand side of Eq. [4] during the ξ - sweep, so that this equation become

$$\xi - \text{sweep} : \quad L_\xi \, (\Delta\tilde{\phi}) = -\alpha R$$

The value of α is given a variation according to geometric sequence defined by

$$\alpha_k = \alpha_{max} \left[\frac{\alpha_{min}}{\alpha_{max}} \right]^{\frac{(k-1)}{(k_n-1)}} \qquad [6]$$

where k = 1,2,3, ..., k_n with k_n represent the number of α_k values to be defined, between 4 to 8. The α_{max} and α_{min} parameters represent the maximum and minimum values of selected α, respectively, which are defined as

$$\alpha_{max} = 1 \quad \text{and} \quad \alpha_{min} = \frac{4}{(\Delta x)^2}$$

where Δx is the grid spacing in the chordwise - direction. It was found that the stability and convergence rate of solutions is strongly depends on the number of cyclic values of α_k being used. For each different case, an investigation has to be made for the definition of an appropriate value of this parameter.

STRUCTURAL MODEL

Structural model used in this work is derived using a finite element representation. Stiffness of the structure is represented by a stiffness beam (cantilever beam) located at the lifitng surface shear center or elastic axis which is assumed to be a straight line. Meanwhile its mass is represented with lump mass located at the section center of gravity and connected to the stiffness beam with a rigid bar. The stiffness beam is divided into at least 20 beam – elements , with 6 (six) degree of freedom (d.o.f) at each of its nodal points.

Mathematical representation of this finite element model can be written as :

$$[K]\{q\} = \{p\} \qquad [7]$$

where [K] represents the beam stiffness matrix , and { q } and { p } are , respectively , represent the vector of generalized coordinate or d.o.f and the generalized aerodynamic force vector. Elements of the aerodynamic force vector is defined as the integral of surface pressure over section area , Ω :

$$\tilde{p}_j = \iint_{\Omega} \Delta p(x,y)\, d\Omega$$

and $$\{p\} = \iint_{\Omega} [N]^T \{\tilde{p}_j\}\, d\Omega \qquad [8]$$

in which [N] represents element matrix of shape function.

Equation [7] is solved iteratively using the aerodynamic load at zero structural deformation as an initial value. This iterative process is shown in the diagram of the following Figure 1. Convergence criteria for each case is that the difference between the deformation at the i-th and (i+1)-th iterations is not more than 10^{-4}.

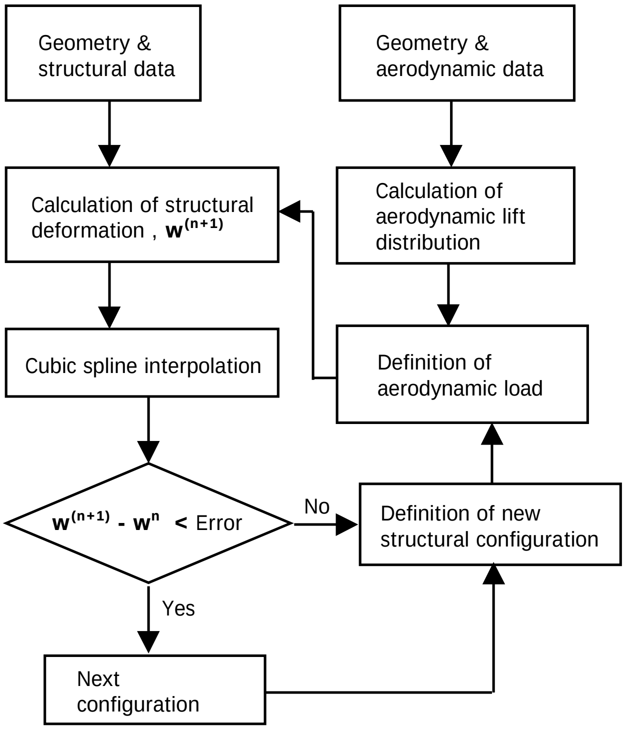

Figure 1. Lift redistribution calculation diagram

NUMERICAL VALIDATION

Validation of the present technique for prediction of aerodynamic lift redistribution is carried out using a clean tapered wing configuration with swept angle of 26.3 degree , aspect ratio of 8.4 and supercritical airfoil . Thickness ratio of the airfoil are 14% at the root , 9.5 % at the kink and 8.5% at the tip. Stiffness (bending and torsional) and mass properties of this wing configuration is shown in Figure 2. In this study , wing structure is devided into 29 sections (30 nodal points) which are assumed to be perfectly rigid in the chordwise direction. The elastic axis of the wing is positioned at 41.05% chord from the wing leading edge.

Analysis of the aerodynamic lift redistribution due to elastic behavior of the wing are carried out at several combination of flow Mach number and wing initial angle of attack , as follow :

a. Mach number , M = 0.2 , 0.4 , 0.6
b. Angle of attack α = 2^o , 4^o , 6^o

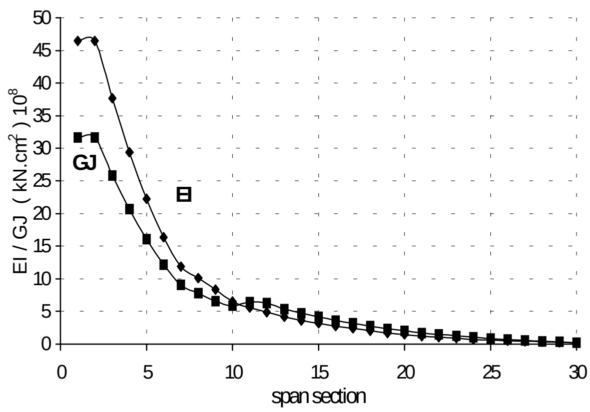

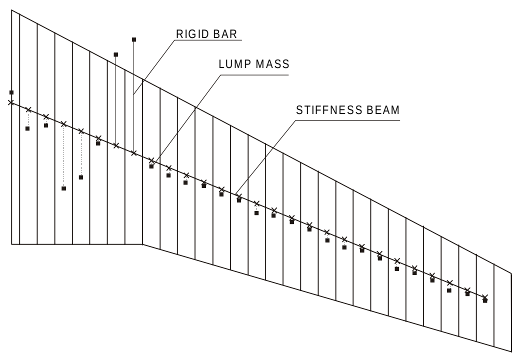

Figure 2. Wing planform and stiffness distribution

Calculation of aerodynamic response using NTRANS is based upon convergence criteria that the error in the total lift coefficient over the wing surface at j-th iteration is less than maximun error defined , which is equal to 10^{-3}. In general , convergence aerodynamic response are obtained at less than 5 iterations. Meanwhile , a total of 3 to 4 iteration are required for the convergence in the calculation of the structural deformation.

Chordwise distribution of lift coefficient at 70% span from the wing root (section - 20 in span direction) for several iteration is shown in Figure 3 and 4. The distribution at each iteration shows the distribution due to the correction in α which is coming from the elastic deformation of the structure. Figure 3 shows the distribution of aerodynamic lift coefficient at flow Mach number M = 0.2 and angle of attack α = 2 , 4 and 6 degree. It can be seen that the aerodynamic lift correction between the first and second iteration is larger compared to the correction between the second and the third iteration . Convergence results for both aerodynamic and elastic deformation is found after the fourth iteration. Special result was seen for α = 6 degree where the lift correction between each iterations are small . This is due to the high angle of attack that the wing torsional stiffness gives significant contribution to the total stiffness of the structure which make the structure less flexible.

In this case the deformation consist of coupling between torsion and bending mode.

Similar results was also found for larger value of angle of attack. At angle of attackj larger than 8 degrees flow solution gives divergence results due to the flow separation which starting to developed on the upper surface. Comparison of these results with the results obtained using USAERO code (which is based upon panel method) for the corrected wing surface geometry shows a reasonably good agreement. Geometry correction given to the wing consist of vertical bending and twist deformation which are obtained from the deformation distribution of the wing structure.

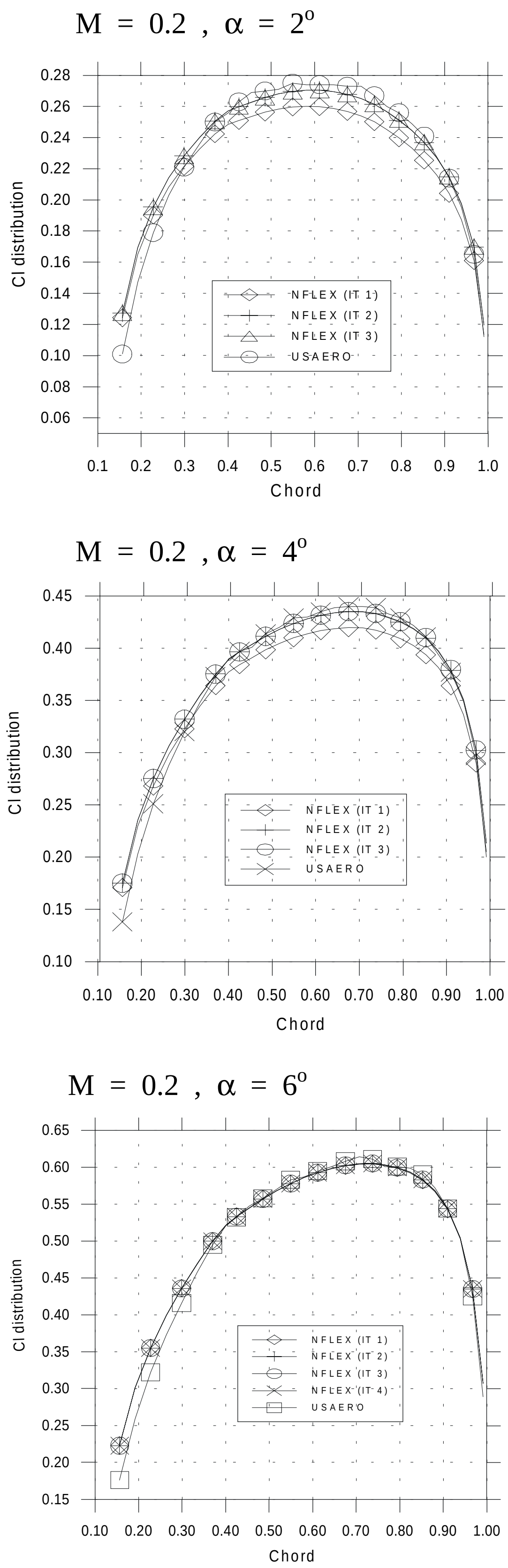

Figure 3. Variation of pressure distribution on the upper surface with initial angle of attack at Mach number M = 0.2

$M = 0.4 \;,\; \alpha = 2^o$

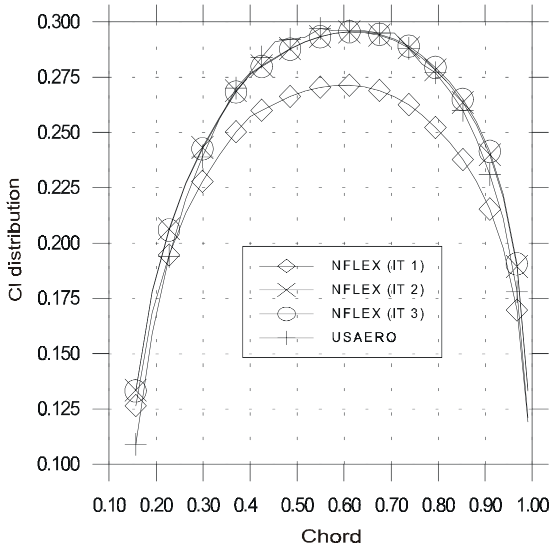

$M = 0.6 \;,\; \alpha = 2^o$

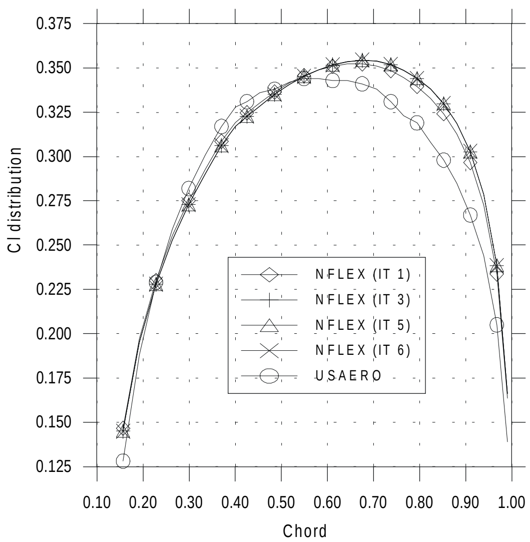

Figure 4. Variation of pressure distribution on the upper surface with Mach number at angle of attack $\alpha = 2^o$

Variation of lift distribution on the upper surface at different flow Mach number are shown in Figure 4. As the free stream Mach number increases , the difference in pressure distribution between the first and the second or the third iteration become more significant, but it still has similar distribution shape. Since the wing has a supercritical airfoil , there is no shock waves developes on the wing surface . But as the free stream Mach number increases , the viscous effects become more significant and can not predicted accurately by the lag-entrainment viscous model implemented in NTRANS code. For rectangular wing with uniform cross section , calculation shows an excellent result even tough there are strong shock waves develope on the wing surface.

Twist distribution along the wing span due to aerodynamic pressure are shown in Figure 5 below. Twist angle are calculated at the elastic axis of the wing section which is positioned at 41.05% chord from the airfoil leading edge. Wing configuration for these calculations is the same as configuration for previous aerodynamic calculations. The structure is given a 2 degree angle of attack and calculation are carried out at free stream Mach number of M = 0.2 , 0.4 , 0.6 and 0.8. Figure 5 shows the comparison of twist distribution results along the wing span between elastic wing and rigid wing . A maximum of 5 iterations are required to obtained the elastic twist distribution. It can be seen that as the free stream Mach number increases (in which the change in aerodynamic lift coefficients due to wing flexibility increase) , the twist angle and angle of attack corrections also increase. Maximum twist along the wing span accur at the wing tip.

Mach Number	Maximum Twist	α Correction
0.2	0.01591^o	0.126^o
0.4	0.07761^o	0.260^o
0.6	0.25707^o	0.528^o
0.8	1.18698^o	1.327^o

Significant twist and angle of attack correction due to structure flexibility was found for free stream Mach number larger than M = 0.6. This is in conjunction with a large change in the aerodynamic lift distribution on the surface .

CONCLUSIONS

A three - dimensional structure and flow solution procedure was developed based upon the solution of nonlinear transonic small disturbance equations couple with linier finite element solutions .

The procedure was applied to determine the redistribution of aerodynamic lift on the wing surface and the distribution of twist angle and also angle of attack correction due to structure flexibility. Numerical results show that the characteristics of the aerodynamic redistribution , twist angle and angle of attack correction are strongly depend upon flexibility distribution of the wing structures , initial angle of attack and free stream Mach number. This procedure is accurate and efficient for routine use in aircraft structural design and analysis.

REFERENCES

[1] Bisplinghoff, R.L. and Ashley, H. : Principle of Aeroelasticity , John Wiley & Sons , New York , 1969.

[2] Tijdeman, H. : Investigation of the transonic flows around oscillating airfoil , National Aerospace Laboratory , NLR TR-77090U , The Netherland , 1978.

[3] Ashley, H. : Role of shocks in the sub-transonic flutter phenomena , AIAA Paper 79-0765 , April 1979.

[4] Albano, E. and Rodden, W.P. : A Doublet - Lattice method for calculating lift distribution on oscillating surfaces in subsonic flows , AIAA Journal , vol. 7 , no. 2 , February 1969 , pp. 279-285.

[5] Tjatra, I W. : Transonic aeroelastic analysis of systems with structural nonlinearities , Ph.D. Thesis , Virginia Tech. , Blackburg , Va. , 1991.

[6] Jameson, A. : Transonic potential flow calculation in conservation form , Proceeding AIAA second Computational Fluid Dynamics Conference , Hartford , Conn. , 1975.

[7] Kwak, D. : Non-reflecting farfield boundary conditions for unsteady transonic flow calculation , AIAA Paper 80-1393 , 1980.

[8] Tjatra, I W. : Application of unit pulse transfer function method in the calculation of nonlinear unsteady transonic generalized aerodynamic forces , Proceeding of the CMSE Conference , Bandung , October 1997.

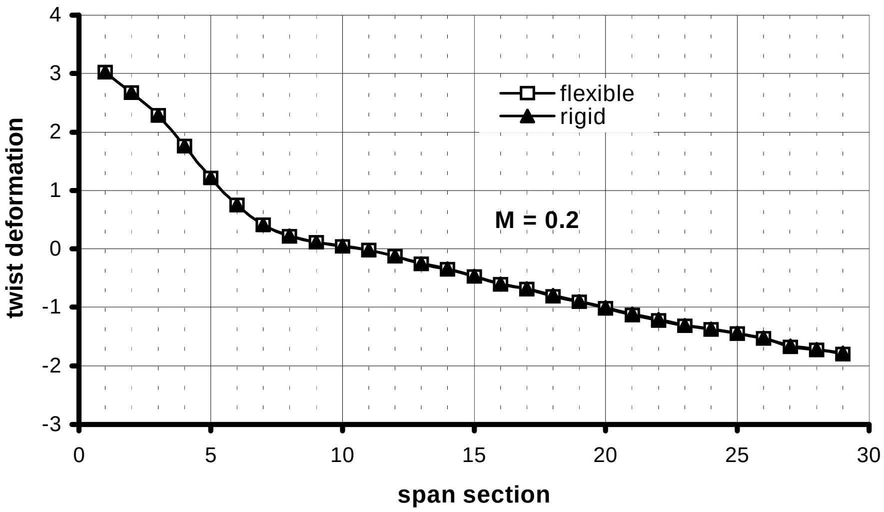

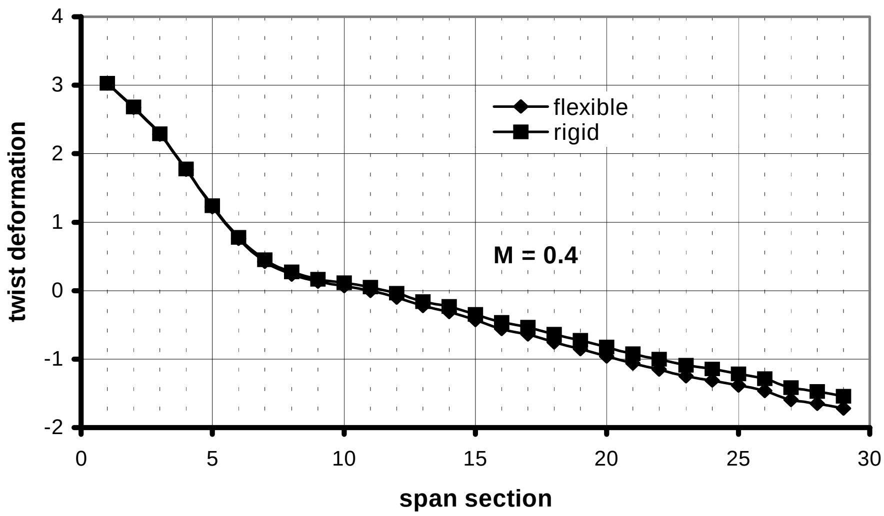

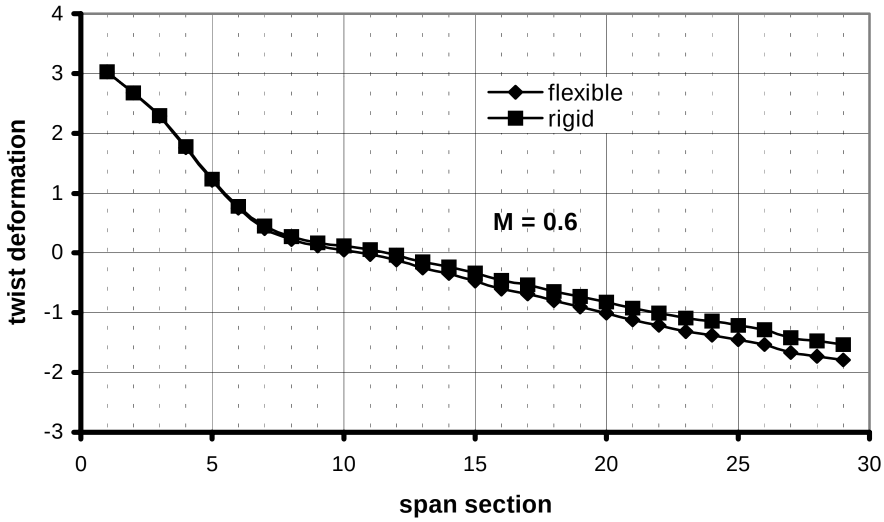

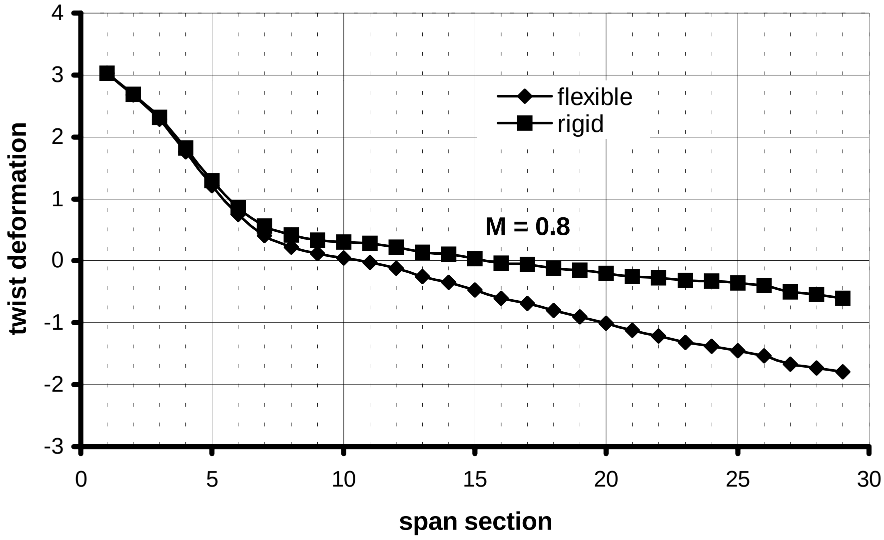

Figure 5 . Variation of spanwise twist distribution with free stream Mach number at initial angle of attack 2^o